The ammonia absorption spectrum between 3900 and 6350 cm-1: 15NH3 contribution and a recommended list for natural ammonia

P. Cacciani, P. Čermák, J. Vander Auwera, A. Campargue

Contents lists available at ScienceDirect

Journal of Quantitative Spectroscopy and Radiative Transfer

journal homepage: www.elsevier.com/locate/jqsrt

The ammonia absorption spectrum between 3900 and 6350 cm^{-1}: $^{15}NH_3$ contribution and a recommended list for natural ammonia

P. Cacciani [a], P. Čermák [b], J. Vander Auwera [c], A. Campargue [d,*]

[a] Laboratoire de Physique des Lasers, Atomes et Molécules, CNRS, UMR 8523 Université Lille, 59655 Villeneuve d'Ascq Cedex, France
[b] Department of Experimental Physics, Faculty of Mathematics, Physics and Informatics, Comenius University, Mlynská dolina F2, 842 48 Bratislava, Slovakia
[c] Spectroscopy, Quantum Chemistry and Atmospheric Remote Sensing (SQUARES), C.P. 160/09, Université Libre de Bruxelles, 50 avenue F.D. Roosevelt, B-1050 Brussels, Belgium
[d] Univ. Grenoble Alpes, CNRS, LIPhy, 38000 Grenoble, France

ARTICLE INFO

Keywords:
Ammonia
NH3
Isotopologue
15NH3
Absorption spectroscopy

ABSTRACT

Following previous contributions dedicated to the main isotopologue, $^{14}NH_3$, in the present work, we examine the $^{15}NH_3$ absorption spectrum between 3950 and 6350 cm^{-1} in order to elaborate an absorption line list for ammonia in natural isotopic abundance. For this purpose, several room temperature Fourier Transform absorption spectra of ammonia highly enriched in $^{15}NH_3$ measured in the 90's and available from the Kitt Peak data centre have been analysed. In addition, a more recent high-resolution spectrum recorded in Brussels between 4150 and 4600 cm^{-1} is also considered. The spectra were divided in three separate intervals (3900–4706, 4706–5650 and 5650–6350 cm^{-1}) for which experimental lists including 3506, 3788, and 2317 lines, respectively, were retrieved and treated independently. By comparison with an *ab initio* line list (the BYTe list) and systematically validating the assignments by using lower state combination difference relations (LSCD), 2013, 1771 and 570 transitions could be assigned in the three regions, respectively. They belong to 16, 22, and 10 bands and correspond to 98.5, 92.6 and 78.6 % of the experimental intensities in the region, respectively. For comparison, only four $^{15}NH_3$ bands were previously assigned in the literature in the entire studied region.

The obtained $^{15}NH_3$ assigned line lists were gathered with the previously elaborated line list of the main isotopologue to produce a recommended line list for natural ammonia between 3900 and 6350 cm^{-1}.

1. Introduction

The present work is a further contribution aiming to improve the knowledge of the absorption spectrum of ammonia in the near infrared. In the last years, we have reported several analyses by Fourier Transform Spectroscopy (FTS) in the 3900–6350 cm^{-1} spectral range (2.56–1.57 μm) [1-4]. Those works were mainly limited to the main isotopologue, $^{14}NH_3$, with most of the weak $^{15}NH_3$ lines being identified and discarded. In order to elaborate a line list for ammonia in natural isotopic abundance, the $^{15}NH_3$ minor isotopologue, with a natural abundance of 3.661×10^{-3}, has to be considered in more detail. Here, we study several isotopically enriched spectra to elaborate a $^{15}NH_3$ line list which will have intensity scaled according to the $^{15}NH_3$ natural abundance and will be gathered with the $^{14}NH_3$ list in order to account for the absorption of natural ammonia. Note that deuterated ammonia, NH_2D, has one order of magnitude smaller abundance than $^{15}NH_3$ (4.35×10^{-4}).

The review of the literature indicates that previous $^{15}NH_3$ observations are limited in the studied region. The most extended study from Urban et al. [6] is forty years old and limited to the 4000–4500 cm^{-1} interval corresponding to the range of the $\nu_1+\nu_2$ band centered at 4288 cm^{-1}. Only relative intensity information is provided in this work. More recently, Čermák et al. re-examined the 4275–4340 cm^{-1} interval by laser absorption spectroscopy using a Vertical External Cavity Surface Emitting Laser (VECSEL) as a light source [5]. Line intensities were retrieved from the spectra and the observations were significantly extended in the studied spectral interval (244 $^{15}NH_3$ lines were assigned instead of about 80 by Urban et al. [6]).

In the present version of the HITRAN database [7], no information is provided for $^{15}NH_3$ in the $\nu_1+\nu_2$ band region. In our region of interest (3900 - 6350 cm^{-1}), only 126 transitions of the $\nu_3+\nu_4$ band centered near 5041 cm^{-1} are provided. Their source is a publication by Brown&Margolis based on FTS spectra recorded in the 90's at the

* Corresponding author.
E-mail address: alain.campargue@univ-grenoble-alpes.fr (A. Campargue).

https://doi.org/10.1016/j.jqsrt.2024.109148
Received 16 July 2024; Accepted 7 August 2024

Table 1
Experimental conditions corresponding to the FTS spectra of ammonia highly enriched in $^{15}NH_3$ analysed in this work.

Label	Kitt Peak file	P (Pa)	L (m)	PL (Pa × m)	T (K)	$^{15}NH_3$ enrichment (%)	Analysed region [a]
R12	900307R0.012	120.0	0.25	30	293.5	93.00	I, II
R16	930826R0.016	266.6	2.4	640	297	96.06	I, II
R17	930826R0.017	694.6	2.4	1667	297	98.40	I, II, III
R18	930826R0.018	1399.8	2.4	3360	297	99.43	II
ULB		4.28[b]	27.6	118	294	94.16	I

Notes.
[a] Spectral intervals of the considered spectrum which were analyzed: I, II and III correspond to the 3950–4706, 4706–5500 and 5650–6350 cm^{-1} intervals, respectively.
[b] Estimated value, see Text.

National Solar Observatory at Kitt Peak [8]. In fact, several FTS spectra recorded in a variety of experimental conditions and isotopic enrichments are available in the Kitt Peak archives. In particular, a few ammonia spectra were recorded with a $^{15}NH_3$ enrichment larger than 90 %. In the present work, we consider four of these $^{15}NH_3$ spectra over the wide 3900–6350 cm^{-1} region. In addition, we use as a complementary source an FTS spectrum recorded in Brussels with an improved frequency sampling in the 4150–4600 cm^{-1} region.

The first step of the analysis is presented in the next section and consists in the retrieval of experimental line parameters, in particular, absolute line intensities. As the studied spectra correspond to three separate band systems, the spectral range was divided into three sections: 3900–4706, 4706–5650, and 5650–6350 cm^{-1}. The next step is the rovibrational assignments described in Section 3. Following the procedure applied to the $^{14}NH_3$ spectra [1-4], the rovibrational assignments rely on the position and intensity agreements with a theoretical line list namely, the BYTe-15 list calculated by Yurchenko [9] available at https://www.exomol.com/. The obtained assignments will be systematically checked and validated by using Lower State Combination Difference (LSCD) relations of the frequencies of the transitions reaching the same upper state energy level.

The final step and main output of the present work is the combination of the $^{15}NH_3$ list with the $^{14}NH_3$ lists of Refs. [2-4] to elaborate a list of transitions of ammonia in natural abundance in the studied region.

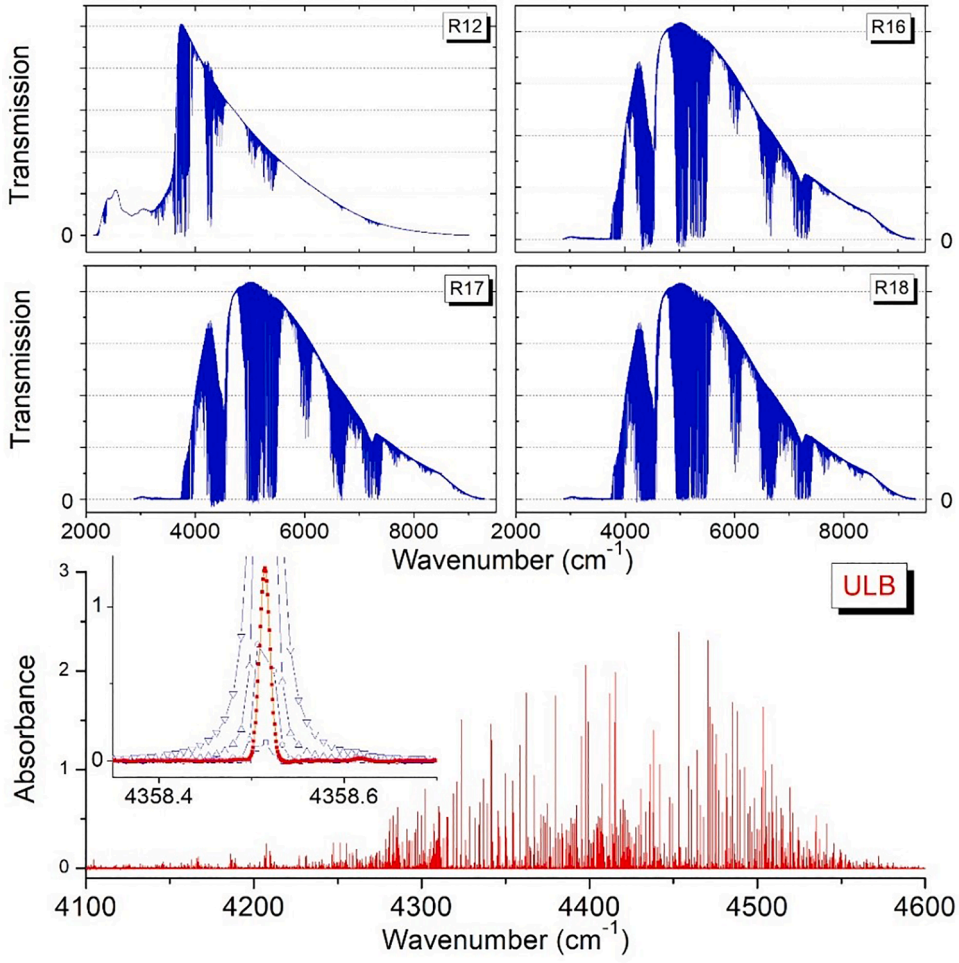

Fig. 1. Overview of the five spectra of ammonia highly enriched in $^{15}NH_3$ analysed in the present work, including four Kitt Peak spectra (blue traces, upper panels) and a spectrum recorded at ULB (red trace, lower panel). The corresponding experimental conditions are given in Table 1. The insert on the lower panel illustrates the better sampling of the line profile provided by the ULB spectrum compared to the Kitt Peak spectra.

The task is straightforward for isolated transitions but requires some extra effort in the case of blended lines involving contributions of both $^{14}NH_3$ and $^{15}NH_3$.

2. Experimental spectra

2.1. Kitt Peak spectra

The four considered Kitt Peak spectra (labeled R12, R16, R17, and R18) are listed in Table 1 which includes the experimental parameters of the recordings. An overview of the four spectra is included in Fig. 1. All the spectra were recorded at room temperature with a very high $^{15}NH_3$ enrichment. The used path lengths (*L*) and pressure values (*P*) lead to *PL* product values ranging over two orders of magnitude (see Table 1). A CO cell was used for the frequency calibration. Atmospheric water lines are observed with a broadened line shape in the 3900–4100 cm^{-1} and 5150–5300 cm^{-1} ranges. The frequency sampling was low (a few spectral points FWHM) which limits the accuracy of the retrieved positions and intensities.

2.2. The ULB spectrum

The considered ULB FTS spectrum was recorded in 2016 for comparison purpose with the results obtained by laser spectroscopy with a VECSEL source [5]. This spectrum offers a better frequency sampling than the Kitt Peak spectra (typically 5 and 30 spectral points FWHM for the Kitt Peak and ULB spectra, respectively – see insert in Fig. 1). The partial pressure of $^{15}NH_3$ (and $^{14}NH_3$) was determined by intensity comparison with Kitt Peak spectra (see below). The relatively small *PL* value of the ULB spectrum (see Table 1) makes it valuable to determine accurately the line parameters of the strongest lines recorded at low pressure. The frequency calibration of the ULB spectrum was performed by using H_2O and $^{14}NH_3$ lines as reference lines.

3. Analysis

3.1. The 3900–4706 cm^{-1} range

All but the R18 spectrum were used to elaborate a global line list in the 3900–4706 cm^{-1} region. The ULB spectrum of better quality but with a limited sensitivity was selected for the line parameter retrieval in the core part (4150 - 4600 cm^{-1}) of this strong absorption region.

Line positions and line intensities were retrieved using a multi-line fit of the spectra. The fit was performed assuming a simple Voigt function as line profile, with the Gaussian component fixed to the Doppler broadening. The Lorentzian component of the Voigt profile, identical for all the lines, was adjusted in the fit. Constraining the line shape helped to disentangle blended lines.

The unknown partial pressures of $^{15}NH_3$ and $^{14}NH_3$ in the ULB sample were determined from the ULB/R16 ratios of the integrated absorbances averaged over the 10^{-22} - 2×10^{-21} cm/molecule intensity range. It leads to a value of 4.03 Pa for the $^{15}NH_3$ partial pressure. To complete the ULB line list in the region, the more sensitive R16 spectrum was used allowing the lowering of the intensity threshold by about a factor of 5. On the low and high energy edges of the region (3900–4150 and 4600–4706 cm^{-1}, respectively), the R17 spectrum with a *PL* value about 14 times larger than that of the ULB spectrum was adopted allowing intensity meaurements down to about 3×10^{-24} cm/molecule in these intervals. We present in Fig. 2 an example of the retrieval of the ammonia line parameters from the R17 spectrum in a region where the weak NH_3 lines are partly obscured by strong lines of atmospheric water vapor showing a much broader profile due to pressure broadening. Finally, the strongest transitions (intensity above 2×10^{-21} cm/molecule) were retrieved from the R12 spectrum to avoid the effect of apparatus function on strong lines observed in Ref. [2].

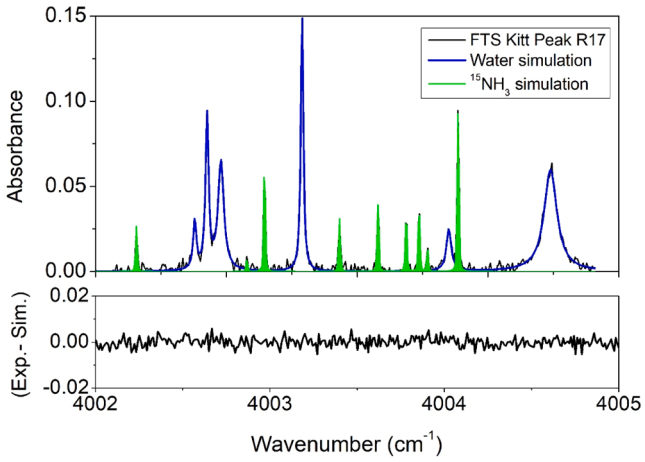

Fig. 2. Illustration of the procedure used to retrieve the $^{15}NH_3$ line parameters from the R17 Kitt Peak spectrum. The displayed spectral interval near 4004 cm^{-1} corresponds to a region where strong absorption lines of atmospheric water vapor partly obscure the weak ammonia lines. On the upper panel, the best fit spectra of water vapor (blue) and ammonia (green) are superimposed to the experimental spectrum (black). The (Exp. –Sim.) residuals are displayed on the lower panel.

A global list of ammonia transitions (thus including both $^{15}NH_3$ and $^{14}NH_3$ transitions) was elaborated in the region and is provided as a first supplementary material. It includes a total of 3506 transitions which are plotted in Fig. 3. The sources of the lines (ULB, R12, R16, or R17) are given in the supplementary material and illustrated in Fig. 3.

The rovibrational assignments followed the same method as the one used for the $^{14}NH_3$ species. The procedure has been described in detail in Refs. [1-4]. The ten years old *ab initio* line list of Ref. [9] (hereafter, the BYTe list) which is available from the ExoMol website (www.exomol.com) was used as a primary source. As in Refs. [1-4], a simplified notation is used for the rovibrational assignments and detailed in the headings of the supplementary material. Note that a new potential energy surface became available for ammonia in 2018 and used to elaborate an improved line list for the main isotopologue [10] (the C2018 list) but the calculations of the corresponding $^{15}NH_3$ list were not available at the date of the completion of the present work.

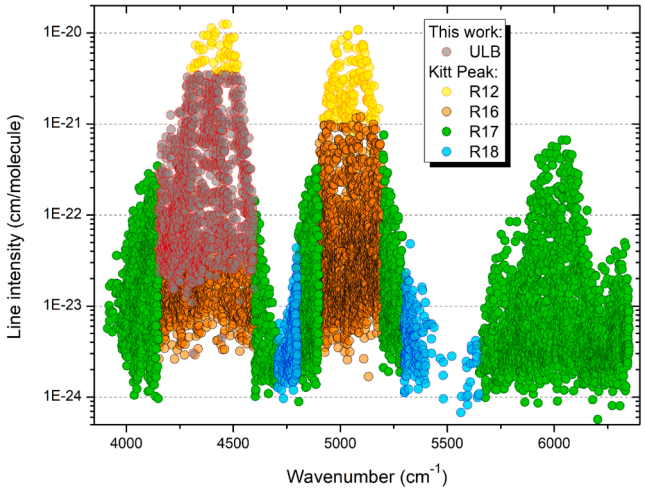

Fig. 3. Overview of the line lists retrieved from ammonia spectra highly enriched in $^{15}NH_3$. The different colored symbols correspond to the five FTS spectra recorded with different experimental conditions (see Table 1) which were used to construct a global line list between 3950 and 6350 cm^{-1}.

Table 2
Statistics and integrated absorption of the various vibrational bands contributing to the $^{15}NH_3$ spectrum between 3900 and 6350 cm^{-1}. The bands are ordered according to their BYTe integrated intensities. The table is organized in three sections corresponding to the 3900-4706, 4706-5650 and 5650-6350 cm^{-1} spectral intervals.

Vibrational state			BYTe			Assigned lines (This work)					
Upper		Lower									
Vib[a]	Sym[b]	*Vib*[a]	E_0 [c] (cm^{-1})	*Nb*[d]	Band Int.[e] (cm/molecule)	Nb [f]	J_{min} /J_{max} [g]	$<\delta>$[h] (cm^{-1})	Int. Sum [i] (cm/molecule)		Int. ratio [j] %
									Exp.	C2018	
011010	E' (3)	000000	4403.63	973	4.101E-19	432	0/16	0.33	3.870E-19	4.080E-19	99.5
011010	E" (6)	000000	4421.49	986	4.034E-19	443	0/16	0.31	3.804E-19	4.015E-19	99.5
110000	A1′ (1)	000000	4307.72	526	6.814E-20	172	1/12	0.15	6.476E-20	6.652E-20	97.6
110000	A2" (5)	000000	4312.30	528	6.515E-20	176	0/14	0.08	6.130E-20	6.377E-20	97.9
021010	E' (3)	010000	4186.11	464	1.111E-20	139	0/11	-1.06	9.483E-21	9.441E-21	85.0
010202	E" (6)	000000	4181.27	837	9.146E-21	144	0/11	0.01	7.242E-21	6.523E-21	71.3
021010	E" (6)	010000	4388.55	435	7.949E-21	98	1/9	0.29	5.173E-21	5.584E-21	70.2
010200	A2" (5)	000000	4161.85	450	7.145E-21	120	0/10	-0.05	7.463E-21	6.165E-21	86.3
010202	E' (3)	000000	4125.66	752	6.897E-21	123	0/10	0.08	6.019E-21	5.128E-21	74.3
010200	A1′ (1)	000000	4126.86	390	5.456E-21	108	1/9	0.18	5.664E-21	4.383E-21	80.3
030101	E" (6)	000000	4506.97	533	1.800E-21	8	8/11	1.07	3.597E-22	3.808E-22	21.1
120000	A1′ (1)	010000	4071.06	193	1.492E-21	40	1/7	-2.43	1.075E-21	9.768E-22	65.5
031010	E' (3)	020000	4226.43	217	5.015E-22	2	4/6	-0.12	1.939E-23	1.336E-23	2.7
040000	A2" (5)	000000	4034.03	131	2.786E-22	6	3/4	-0.32	5.671E-23	4.756E-23	17.1
011111	E' (3)	000101	4389.53	163	1.442E-22	1	3/3	-0.37	2.735E-23	2.248E-23	1.6
100101	E" (6)	010000	4006.26	95	8.377E-23	1	6/6	-0.26	1.090E-23	9.711E-24	11.6
Total				**7673**	**9.990E-19** [k]	**2013**			**9.360E-19**	**9.784E-19** [k]	**97.9** [k]
001111	E' (3)	000000	5041.33	1290	3.246E-19	455	0/13	-0.12	3.212E-19	3.184E-19	98.1
001111	E" (6)	000000	5041.94	1265	3.225E-19	444	0/13	-0.16	3.142E-19	3.135E-19	97.2
001111	A2" (5)	000000	5058.75	508	1.546E-20	55	4/9	-1.26	8.798E-21	8.443E-21	54.6
001111	A1′ (1)	000000	5040.00	526	1.545E-20	69	3/10	-1.12	1.040E-20	1.008E-20	65.2
100101	E' (3)	000000	4949.83	908	1.458E-20	162	0/9	-0.65	1.569E-20	1.122E-20	76.9
100101	E" (6)	000000	4950.85	899	1.372E-20	147	0/9	-0.53	1.405E-20	9.787E-21	71.3
040101	E' (3)	000000	5076.73	532	7.221E-21	1	4/4	-1.03	5.191E-22	4.260E-22	5.9
001111	A2′ (2)	000000	5040.00	506	7.163E-21	35	3/10	0.23	4.523E-21	4.478E-21	62.5
001111	A1" (4)	000000	5058.75	496	6.609E-21	56	3/11	0.19	5.201E-21	4.692E-21	71.0
011111	E' (3)	010000	5052.25	384	4.536E-21	99	0/11	-0.21	3.724E-21	3.510E-21	77.3
011111	E" (6)	010000	5075.42	405	3.530E-21	78	0/10	-0.45	2.735E-21	2.480E-21	70.2
021010	E' (3)	000000	5130.70	613	3.011E-21	53	3/11	-0.75	1.265E-21	1.222E-21	40.6
120000	A1′ (1)	000000	5015.65	379	2.253E-21	21	2/7	-2.17	8.892E-22	9.379E-22	41.6
020200	A2" (5)	000000	5074.97	300	1.930E-21	7	3/3	0.18	1.020E-21	5.592E-22	29.0
020202	E" (6)	000000	5094.59	288	1.805E-21	6	5/6	1.09	5.218E-22	3.527E-22	19.5
021010	E" (6)	000000	5333.14	509	9.726E-22	58	1/8	0.32	3.530E-22	3.357E-22	34.5
031010	E' (3)	010000	4889.16	201	3.199E-22	16	1/8	-0.12	1.277E-22	8.588E-23	26.8
011111	A2" (5)	010000	5086.14	110	1.476E-22	1	4/4	0.40	1.602E-23	9.228E-24	6.3
011111	A2′ (2)	010000	5046.32	82	1.208E-22	1	7/7	-0.04	1.335E-23	8.008E-24	6.6
011111	A1" (4)	010000	5052.25	99	9.875E-23	1	5/5	0.62	7.557E-24	6.880E-24	7.0
130000	A1′ (1)	000000	5742.02	30	4.401E-23	4	3/5	-1.79	1.070E-23	1.234E-23	28.0
130000	A1′ (1)	010000	4797.42	53	3.878E-23	2	3/6	-1.92	7.094E-24	5.470E-24	14.1
Total				**10383**	**7.462E-19** [l]	**1771**			**7.053E-19**	**6.905E-19** [l]	**92.5** [l]
011111	E' (3)	000000	5996.84	601	2.039E-20	199	0/12	-0.05	1.841E-20	1.905E-20	93.4
011111	E" (6)	000000	6020.01	705	1.965E-20	198	0/11	-0.31	1.715E-20	1.782E-20	90.7
031010	E' (3)	000000	5833.75	481	2.673E-21	103	1/8	-0.04	2.206E-21	2.016E-21	75.4
011111	A2" (5)	000000	6030.73	272	1.015E-21	6	4/5	0.44	2.614E-22	1.834E-22	18.1
031010	E" (6)	000000	6302.67	216	1.000E-21	29	1/6	1.68	4.213E-22	4.588E-22	45.9
011111	A1′ (1)	000000	5990.91	259	9.037E-22	4	7/7	1.67	4.388E-23	3.029E-23	3.4
011111	A2′ (2)	000000	5990.91	205	7.086E-22	8	4/7	0.27	2.675E-22	2.289E-22	32.3
011111	A1" (4)	000000	5996.84	253	6.674E-22	11	3/5	0.55	1.684E-22	1.817E-22	27.2
021111	E' (3)	010000	5755.46	198	4.821E-22	5	2/5	-2.02	4.702E-23	4.413E-23	9.2
130000	A1′ (1)	000000	5742.02	115	4.471E-22	7	3/6	-1.75	1.025E-22	9.961E-23	22.3
Total				**3305**	**4.794E-20** [m]	**570**			**3.908E-20**	**4.012E-20** [m]	**83.7** [m]

Notes

[a] Vibrational labeling: $V_1V_2V_3V_4L_3L_4$ where V_i = 1-4 are the vibrational normal mode quantum numbers corresponding to the ν_1 symmetric stretch, ν_2 symmetric bend, ν_3 the antisymmetric stretch, ν_4 antisymmetric bend, respectively. $L_3 = |l_3|$ and $L_4 = |l_4|$ are the vibrational angular momentum quantum numbers of the ν_3 and ν_4 modes, respectively

[b] Vibrational symmetry of the upper state with the corresponding index in the D3h(M) symmetry group (1:A1′, 2:A2′, 3:E'; 4:A1", 5:A2", 6:E")

[c] Energy of the lowest level of the upper vibrational state (corresponding generally to $J = K = 0$) as calculated in the BYTe list [9]. In the case of the hot bands, the $J = K = 0$ value of the lowest state was subtracted.

[d] Number of lines of the corresponding band with Byte intensity larger than 1×10^{-25} cm/molecule.

[e] Sum of the BYTe intensities larger than 2×10^{-25} cm/molecule for the considered band

[f] Number of lines of the corresponding band assigned in the studied spectra

[g] Minimum and maximum values of the rotational quantum numbers of the assigned lines

[h] Average value of the (exp.- BYTe) position differences of the considered band

[i] Sum of the intensities of the assigned transitions of the corresponding band

[j] Ratio of the sum of the BYTe intensities of the transitions assigned by the total BYTe of the considered band.

[k] For comparison, the assigned transitions correspond to 97.8 % of the sum of all the BYTe intensities greater than 2×10^{-25} cm/molecule in the 3900-4706 cm^{-1} interval (1.00×10^{-18} cm/molecule).

[l] For comparison, the assigned transitions correspond to 91.8 % of the sum of all the BYTe intensities greater than 2×10^{-25} cm/molecule in the 4706-5650 cm^{-1} interval (7.519×10^{-19} cm/molecule).

[m] For comparison, the assigned transitions correspond to 75.4 % of the sum of all the BYTe intensities greater than 2×10^{-25} cm/molecule in the 5650-6350 cm^{-1} interval (5.317×10^{-20} cm/molecule).

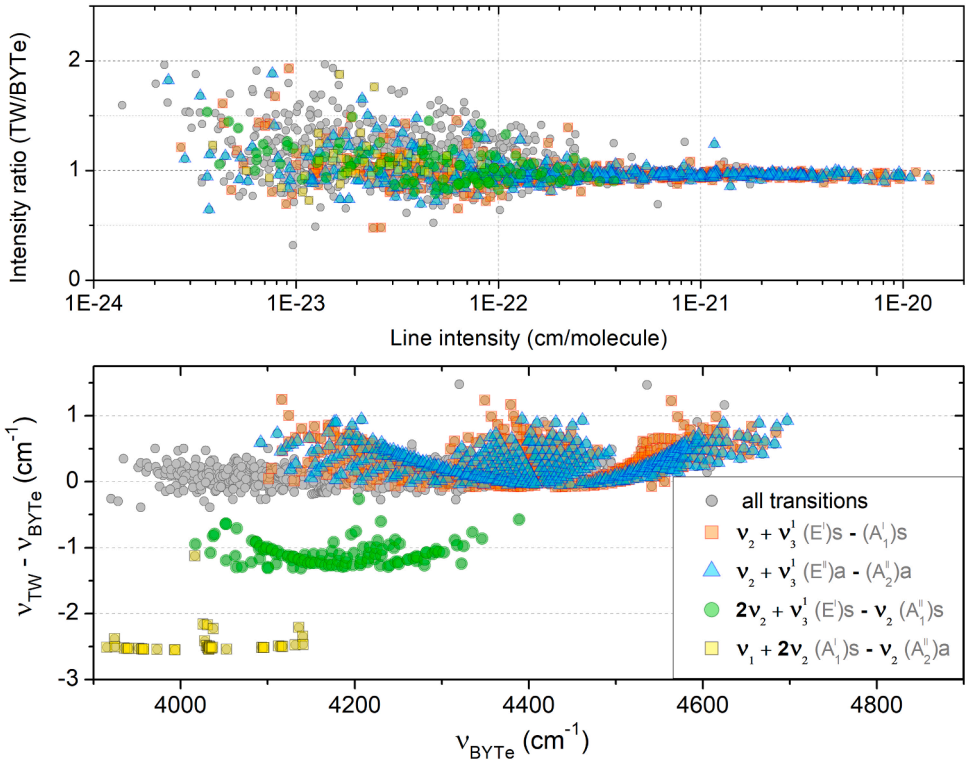

Fig. 4. Position and intensity comparisons between the experimental and the BYTe predictions for $^{15}NH_3$ in the 3900–4703 cm^{-1} range. Four bands are highlighted with different colored symbols.

Based on the agreement of the line parameters (positions and intensities), the correspondence between the experimental and the BYTe transitions were found and validated only when the so-called LSCD (Lower State Combination Difference) relations were fulfilled. The LSCD method relies on the coincidence between the differences in the experimental frequencies of transitions sharing the same upper state and the difference of the energies of their lower states. Accurate lower state energy values were taken from Refs. [11,12] for the ground vibrational state and from Ref. [13] for the V_2= 1, 2, and V_4= 1 states. These values are provided in the assigned line list and coincide with HITRAN values within a few 10^{-4} cm^{-1}. Note that our criterion to validate the LSCD relations was an agreement within typically 3×10^{-3} cm^{-1} between the measured position differences and the difference of the lower state energies.

The $^{14}NH_3$ lines are generally weak due to the abundance of a few % in the studied spectra (see Table 1). Their identification relies on the comparison with our $^{14}NH_3$ line list of Ref. [2]. Finally, 2013 transitions were assigned to $^{15}NH_3$, 504 to $^{14}NH_3$ and 989 lines remain unassigned. Among the 875 $^{15}NH_3$ transitions with an intensity above 1×10^{-21} cm/molecule, only three remain unassigned. The accidental spectral interference between a $^{15}NH_3$ transition and a $^{14}NH_3$ transition was carefully examined to avoid biases on the retrieved $^{15}NH_3$ line intensities.

The obtained $^{15}NH_3$ assignments together with the corresponding BYTe line parameters are included in the experimental list provided as supplementary material. The list includes the identification of the $^{14}NH_3$ lines, except for the weakest lines with intensity below 6.5×10^{-23} cm/molecule. Overall, the $^{15}NH_3$ transitions belong to sixteen vibrational bands including six hot bands listed in Table 2. This table presents band-by-band statistics and intensity comparison to the BYTe list. All unassigned lines have an intensity smaller than 3.77×10^{-22} cm^{-1} cm/molecule, to be compared to intensities of 1×10^{-20} cm/molecule for the strongest lines in the studied region. The $^{15}NH_3$ assigned transitions represent 98.5 % and 97.7 % of the total experimental and BYTe intensities of $^{15}NH_3$ in the region, respectively. In the case of the $\nu_2+\nu_3$ band which is the dominant band of the region, the assigned transitions (up to J_{max}= 15) represent about 99.5 % of the band intensity. Obviously, this percentage decreases with the intensity of the bands (see Table 2).

An overview of the position and intensity comparisons between the observations and the BYTe predictions is presented in Fig. 4. The overall agreement is very good for the intensities except for a systematic overestimation of the BYTe values limited to about 4 %, mostly independent of the band. As concerns positions, all but the $2\nu_2+\nu_3-\nu_2$ and $\nu_1+2\nu_2-\nu_2$ hot bands show a similar behavior: the vibrational shift is limited to ±0.3 cm^{-1} and the rotational structure of the different bands shows deviations smoothly increasing with the rotational excitation (up to 1 cm^{-1} in the case of the $\nu_2+\nu_3$ band). For an unknown reason, the $2\nu_2+\nu_3-\nu_2$ and $\nu_1+2\nu_2-\nu_2$ hot bands appear to be outliers due to a large overestimation of the BYTe vibrational term value on the order of 1.2 and 2.5 cm^{-1}, respectively. The average value of the (exp. - BYTe) position differences is given in Table 2 for each band. In the case of the main isotopologue studied in the same region in Ref. [2], the positions comparison to the more recent C2018 *ab initio* predictions indicates a slightly better agreement. For instance, the average position shift of the $\nu_2+\nu_3$ band (erroneously noted as $3\nu_2+\nu_3$ band in Table 2 of Ref. [2]) is

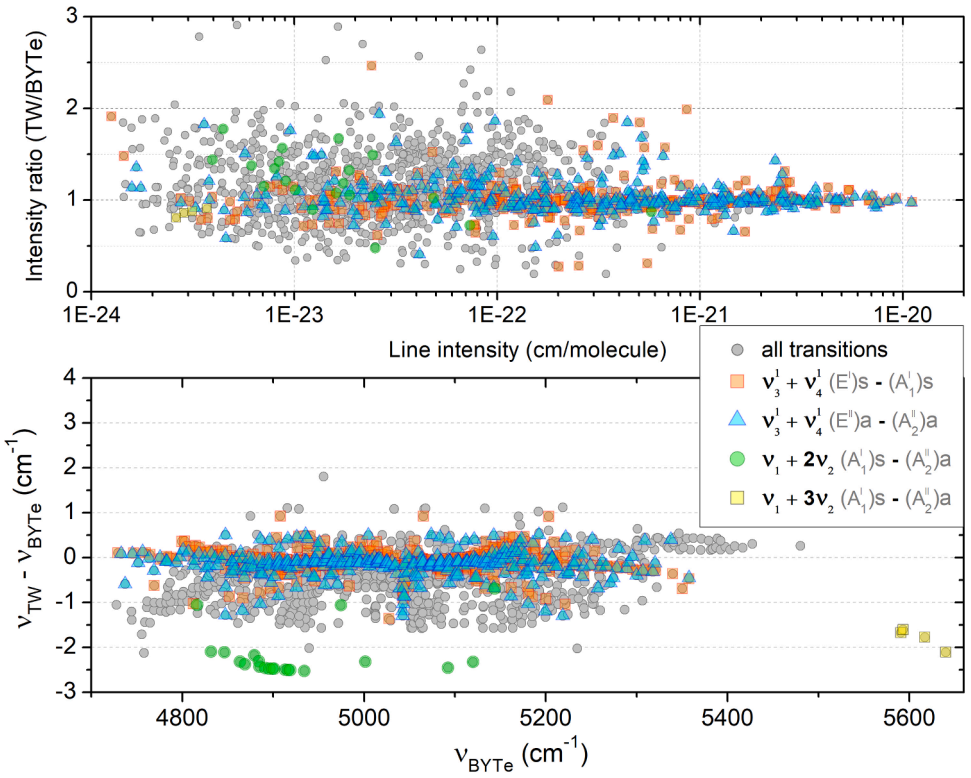

Fig. 5. Position and intensity comparisons between the experimental and the BYTe predictions for $^{15}NH_3$ in the 4706–5650 cm^{-1} range. Four bands are highlighted with different colored symbols.

only 0.08 cm^{-1} for the $^{14}NH_3$ compared to C2018 while it is about 0.28 cm^{-1} for $^{15}NH_3$ (compared to BYTe). Note that in the considered region, the $^{15}NH_3$ bands are isotopically shifted to lower energy by values up to about 20 cm^{-1} compared to the corresponding $^{15}NH_3$ bands.

3.2. *The 4706–5650 cm^{-1} region*

Only the Kitt Peak spectra were used in this range. Depending on the $P \times L$ product (see Table 1), for each intensity range, the most suitable

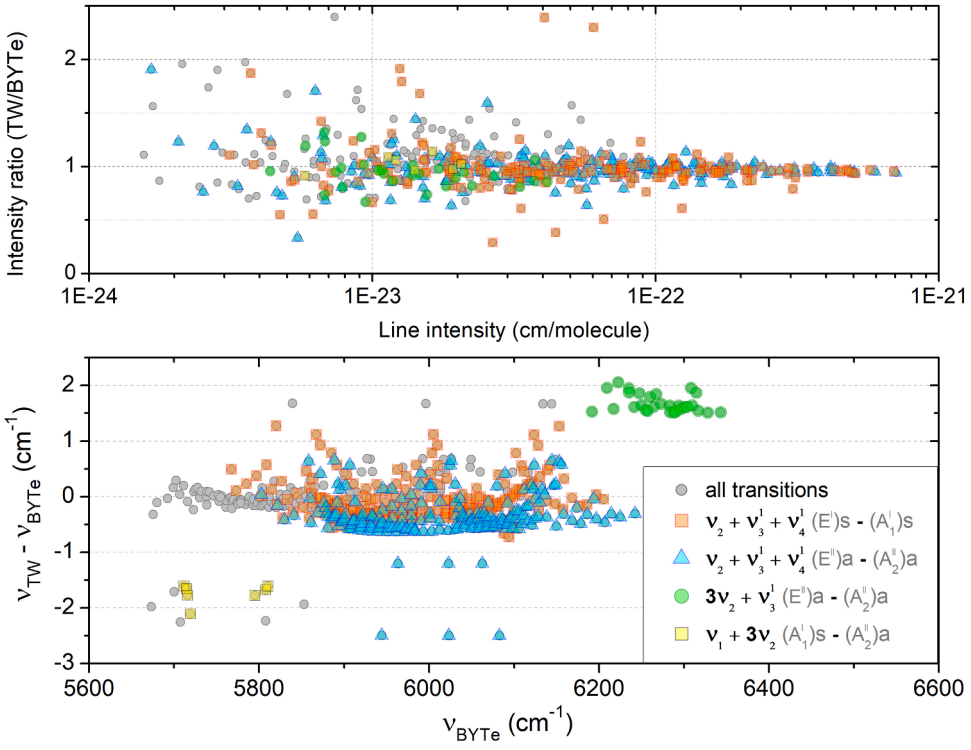

Fig. 6. Position and intensity comparisons between the experimental and the BYTe predictions for $^{15}NH_3$ in the 5650–6350 cm^{-1} range. Four bands are highlighted with different colored symbols.

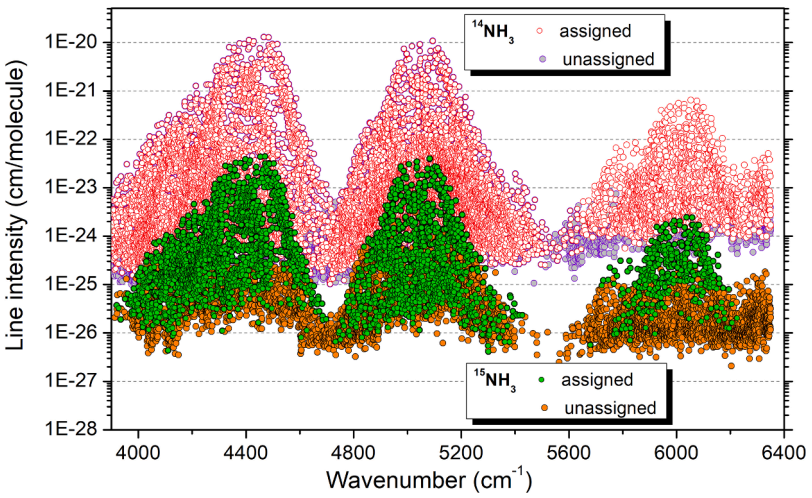

Fig. 7. Overview of the $^{14}NH_3$ and $^{15}NH_3$ line lists included in our recommended line list for natural ammonia between 5650 and 6350 cm^{-1}. Different colours are used for the assigned and unassigned transitions. The $^{14}NH_3$ line list is based on the analysis of Refs. [2-4]. The $^{15}NH_3$ line list, elaborated in the present work, has intensity scaled according to the $^{15}NH_3$ natural abundance.

spectrum was used for the line parameter retrieval (see Fig. 3). In the central part of the region (4900–5200 cm^{-1}), the R12 spectrum was used for the strongest lines with intensity larger than 1×10^{-21} cm/molecule and the R16 spectrum for the others. In the low and high energy regions of weaker absorption, the R17 was adopted for the 4800–4900 and 5200–5300 cm^{-1} intervals while the most sensitive R18 spectrum was used as source in the 4706 - 4800 and 5300 - 5650 cm^{-1} regions. In the latter interval, the retrieval of the ammonia line parameters was hampered by the spectral interference with strong atmospheric lines of water vapor. These water vapor lines were identified and fitted using an air-broadened Voigt profile in order to determine reliable values of the parameters of the $^{15}NH_3$ lines located in the region (as illustrated in Fig. 2). The consistency between the intensity values derived from the different spectra was systematically checked and an average agreement better than 10 % was generally achieved.

A final list of 3788 lines was gathered from the different sources and is included in the supplementary material. It includes a total of 235 $^{14}NH_3$ lines which are marked in the list. Following the above described assignment procedure, 1771 $^{15}NH_3$ transitions were assigned to twenty-two bands listed in Table 2. Overall, 1782 lines remain unassigned. The assigned transitions correspond to 92.9 and 91.8 % of the total experimental and BYTe intensities in the region, respectively. The strongest band of the region is the $\nu_3+\nu_4$ band near 5041 cm^{-1} for which the intensity sum of the assigned transitions represents about 97 % of the total band intensity (see Table 2). The position differences and intensity ratios displayed on Fig. 5 show less regular behavior than in the first region, possibly due to the increased impact of rovibrational interactions at higher energy.

3.3. *The 5650–6350 cm^{-1} region*

In this spectral region of lower absorption, the dominant band is the $\nu_2+\nu_3+\nu_4$ band near 6000 cm^{-1}. An experimental list of 2317 lines was retrieved from the R17 spectrum (see Fig. 3) and is included in the global list provided as supplementary material. It includes about 59 lines of $^{14}NH_3$ and we assigned 570 $^{15}NH_3$ lines, 1688 remains unassigned. The overview comparison presented in Fig. 6 illustrates a vibrational shift on the order of 0.5 cm^{-1} for the $\nu_2+\nu_3+\nu_4$ band and a difference with the BYTe intensities on the order of a few %. Similar to what was observed in the first region, two bands involving at least two quanta of the ν_2 vibration are shifted.

4. Empirical energy levels and recommended line list for natural ammonia in the 3950–6350 cm^{-1} region

The upper state empirical energies of 1560 $^{15}NH_3$ rovibrational levels were derived from the assigned list by adding the lower state energies from Refs. [11-13] to the measured line positions. The complete list of energy levels is given in a separate supplementary material and includes, together with the BYTe assignment and energy value, the (trimmed) average empirical value, the number of transitions used for the energy derivation (up to 9), and corresponding standard deviation. An average *rms* value of 4.0×10^{-4} cm^{-1} with a spread of 5.1×10^{-4} cm^{-1} is obtained for the entire set of determined energy levels. These values give an estimation of the average precision and consistencies of our line centre determinations.

The identified $^{14}NH_3$ transitions were removed from the experimental lists and the intensities were scaled according to the natural abundance value of 3.661×10^{-3}. The resulting $^{15}NH_3$ list is displayed on Fig. 7 where assigned and unassigned transitions are plotted with different symbols.

In our three recent studies of natural ammonia covering the three absorption regions of the 3950- 6350 cm^{-1} range [2-4], $^{15}NH_3$ transitions were partially identified. The present study dedicated to $^{15}NH_3$ allows

Table 3
Amount of assignments and intensity comparison between experiment and theory in the three studied regions.

Range (cm^{-1})	Number of transitions Assigned/Total		Ratio of the sums of the experimental intensities, Assigned/Total		Ratio of the sums of the intensities of the assigned transitions, Experimental/*ab initio*
	$^{14}NH_3$	$^{15}NH_3$	$^{14}NH_3$	$^{15}NH_3$	$^{15}NH_3$
3900–4706	6132/7638 [2]	2013/3002	99.8 [2]	98.5	95.6 %
4706–5650	6560/86292 [3]	1771/3553	99.5 [3]	92.9	102.0 %
5650–6350	2563/4924 [4]	570/2258	95.3 [4]	78.6	97.4 %

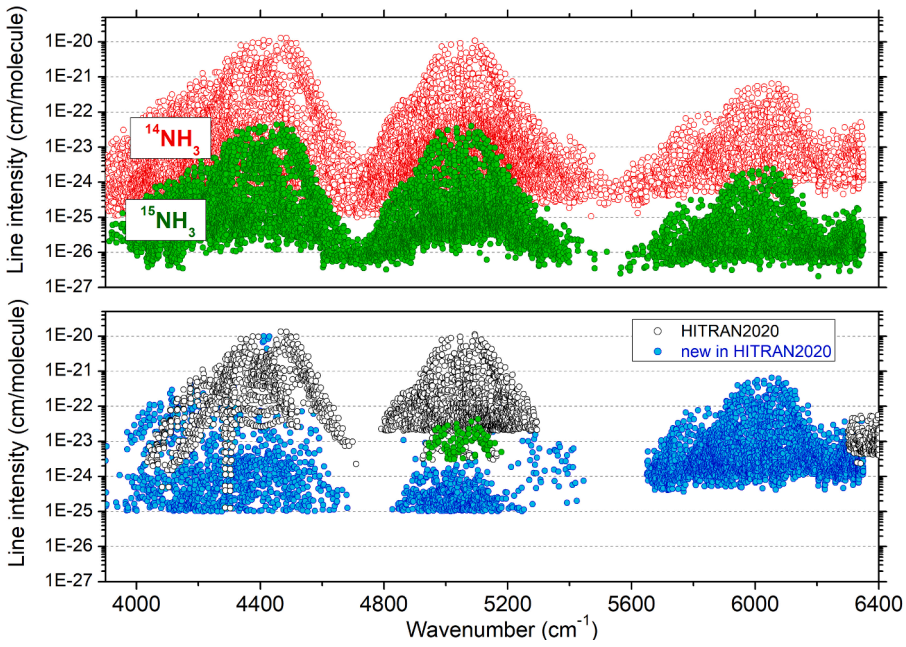

Fig. 8. Overview comparison of the HITRAN2020 line list of ammonia to our recommended line list between 3900 and 6350 cm^{-1}. On both panels, the green symbols correspond to the $^{15}NH_3$ isotopologue. The $^{14}NH_3$ transitions newly included in the 2020 version of HITRAN line list (lower panel, blue circles) include ab initio transitions with position adjusted according to the MARVEL energy of their lower and upper states below 5500 cm^{-1} and a recent analysis of a Kitt Peak spectrum in the 5650 and 6350 cm^{-1} region [1].

for a better treatment and subtraction of the $^{15}NH_3$ contribution to the spectra of Refs. [2-4]. Our $^{14}NH_3$ lists assigned in Refs. [2-4] were derived from FTS spectra recorded at ULB with ammonia samples with natural or slightly $^{15}NH_3$ enriched isotopic abundances. All the $^{15}NH_3$ lines presently measured should be present in those lists if their intensities scaled according to $^{15}NH_3$ abundance are larger than the 10^{-25}–10^{-24} cm/molecule detectivity threshold of the studies of Refs. [2-4]. These $^{15}NH_3$ lines have been systematically searched and removed to get a list of transitions limited to $^{14}NH_3$. Their removal is straightforward for isolated lines but for lines involving a contribution of both $^{14}NH_3$ and $^{15}NH_3$, a new line profile fitting was required and led to a decrease of the intensity of a few tens of $^{14}NH_3$ lines. Overall, in the three absorption regions corresponding to Refs. [2-4], the (laborious) removal procedure of the weak $^{15}NH_3$ lines, was systematically applied down to an intensity threshold of 2.7×10^{-24}, 1.3×10^{-24} and 2.8×10^{-25} cm/molecule leading to the identification and removal of 653, 600 and 327 $^{15}NH_3$ lines, respectively. Some $^{15}NH_3$ contribution remains below these thresholds but the corresponding lines are among the weakest measured in the spectra of Refs. [2-4].

In the case of assigned transitions, for both $^{14}NH_3$ and $^{15}NH_3$, we include in the supplementary material the transition frequencies calculated using our empirically determined value of the upper state energy. These values are expected to be slightly more accurate than the line centre directly determined from the spectra.

The resulting $^{14}NH_3$ line list covering the 3900–6350 cm^{-1} range includes 21,300 lines. The 15,256 assigned $^{14}NH_3$ lines are highlighted in Fig. 7. The statistics of the $^{14}NH_3$ and $^{15}NH_3$ assignments are detailed in Table 3 for the three studied regions. It shows that most of the absorption lines have been assigned in the three regions. Overall, the assigned lines correspond to 99.2 % of the total measured intensities in the region. Compared to *ab initio* calculations, no systematic deviation is evidenced in the three regions.

Due to the abundance scaling factor, depending on the spectra region, the smallest $^{15}NH_3$ intensities are between one and two orders of magnitude below the smallest $^{14}NH_3$ intensities. It is worth mentioning that while the $^{15}NH_3$ lines were carefully removed from the lists assigned in Refs. [2-4], NH_2D lines are probably present among the sets of unassigned transitions of Refs. [2-4], at least in the two most absorbing regions near 4400 and 5000 cm^{-1}. NH_2D has a natural relative abundance of 4.35×10^{-4} which leads to intensities on the order of 5×10^{-24} cm/molecule for the strongest transitions in these two regions, largely above the $^{14}NH_3$ intensity cut-off on the order of 10^{-25} cm/molecule.

5. Concluding remarks

An overview comparison of our ammonia list to the present version of the NH_3 list in the HITRAN database is presented in Fig. 8. Compared to the preceding HITRAN2016 list (black circles on the lower panel), the HITRAN2020 list [7] has been extended by adding calculated $^{14}NH_3$ transitions when both the upper and lower states energies were known from experiment. This approach leads to an unusual appearance below 5300 cm^{-1}, with the inclusion of a large number of hot band transitions with intensities as low as 10^{-25} cm/molecule while the detectivity threshold of the cold band observed in the region (from Urban et al. [6] and Brown&Margolis [8]) is more than two orders of magnitude higher. In the 5650–6350 cm^{-1} range, our analysis of a Kitt Peak spectrum has been adopted as source for HITRAN2020. Very recently, we have improved the analysis of this spectral region using an ULB spectrum of better quality [4]. In the two spectral regions below 5500 cm^{-1}, the ULB spectra at disposal allowed for an improvement of the HITRAN line list which has been discussed in Refs. [2,3]. Regarding the $^{15}NH_3$ species, as mentioned above, the HITRAN2020 list provides only 126 transitions of the $\nu_3+\nu_4$ band centered near 5041 cm^{-1} from Brown&Margolis [8]. We have performed a line-by-line intensity comparison of our measurement to HITRAN data. Excluding three transitions (at 4985.3563, 5044.0873, 5103.8809 cm^{-1}) for which HITRAN intensity is overestimated by about a factor of 3, a difference limited to 5.0 % is obtained for the intensity sum of the 123 remaining transitions, HITRAN value being smaller than our value. The same comparison of our intensity values to the BYTe intensities gives a nearly perfect agreement with a difference smaller

than 1 %.

In summary, we believe that the presently elaborated ammonia line list provides a significant improvement compared to the HITRAN2020 list. The improvements concern the completeness, the accuracy of the line parameters, and the extension of the rovibrational assignments. The latter are necessary to account for the temperature dependence of the line intensities. Further extensions of the line list by adding $^{14}NH_3$ and $^{15}NH_3$ transitions from the C2018 [10] and BYTe [9] lists are possible. In the same way, as done for HITRAN2020, *ab initio* transitions with positions with experimental accuracy can be added when the energy values of the lower and upper states have been experimentally determined.

CRediT authorship contribution statement

P. Cacciani: Formal analysis, Investigation. **P. Čermák:** Methodology. **J. Vander Auwera:** Investigation, Methodology. **A. Campargue:** Investigation, Writing – review & editing.

Declaration of competing interest

The authors declare that they have no known competing financial interests or personal relationships that could have appeared to influence the work reported in this paper.

Data availability

The data are provided as supplementary materials.

Acknowledgements

This research was supported by the Slovak Research and Development Agency (contract no APVV-23-0522) and by the Slovak Grant Agency for Science VEGA (contract no 1/0710/24). This work was also a contribution to the CPER research project CLIMIBIO. The authors thank the French Ministère de l'Enseignement Supérieur et de la Recherche, the Hauts de France Region and the European Funds for Regional Economic Development for their financial support to this project.

Supplementary materials

Supplementary material associated with this article can be found, in the online version, at doi:10.1016/j.jqsrt.2024.109148.

References

[1] Cacciani P, Čermák P, Béguier S, Campargue A. The absorption spectrum of ammonia between 5650 and 6350 cm^{-1}. *J.* Quant Spectrosc Radiat Transf 2021; 258:107334. https://doi.org/10.1016/j.jqsrt.2020.107334.

[2] Cacciani P, Čermák P, Vander Auwera J, Campargue A. The ammonia absorption spectrum between 3900 and 4700 cm^{-1}. *J.* Quant Spectrosc Radiat Transf 2022; 277:107961. https://doi.org/10.1016/j.jqsrt.2021.107961.

[3] Cacciani P, Čermák P, Vander Auwera J, Campargue A. The ammonia absorption spectrum between 4700 and 5650 cm^{-1}. *J.* Quant Spectrosc Radiat Transf 2022; 292:108250. https://doi.org/10.1016/j.jqsrt.2022.108350.

[4] Cacciani P, Čermák P, Votava O, Vander Auwera J, Campargue A. The ammonia absorption spectrum revisited between 5650 and 6350 cm^{-1}. Molec Phys 2023;122 (7–8). https://doi.org/10.1080/00268976.2023.2256893.

[5] Čermák P, Hovorka J, Veis P, Cacciani P, Cosléou J, El Romh J, et al. Spectroscopy of $^{14}NH_3$ and $^{15}NH_3$ in the 2.3 μm spectral range with a new VECSEL laser source. J Quant Spectrosc Radiat Transf 2014;137:13–22. https://doi.org/10.1016/j.jqsrt.2014.01.005.

[6] Urban Š, Misra P, Naharahi Rao K. the $\nu_1+\nu_2$ and $\nu_1+\nu_2-\nu_2$ bands of $^{14}NH_3$ and $^{15}NH_3$. J Mol Spectrosc 1985;114:377–94. https://doi.org/10.1016/0022-2852(85)90233-4.

[7] Gordon IE, Rothman LS, Hargreaves RJ, Hashemi R, Karlovets EV, Skinner FM, et al. The HITRAN2020 molecular spectroscopic database. J Quant Spectrosc Radiat Transf 2022;277:107949. https://doi.org/10.1016/j.jqsrt.2021.107949.

[8] Brown L, Margolis J. Empirical line parameters of NH_3 from 4791 to 5294 cm^{-1}. J Quant Spectrosc Radiat Transf 1996;56:283–94. https://doi.org/10.1016/0022-4073(96)00041-6.

[9] Yurchenko SN. A theoretical room-temperature line list for $^{15}NH_3$. J Quant Spectrosc Radiat Transf 2015;152:28–36. https://doi.org/10.1016/j.jqsrt.2014.10.023.

[10] Coles PA, Ovsyannikov RI, Polyansky OL, Yurchenko SN, Tennyson J. Improved potential energy surface and spectral assignments for ammonia in the near-infrared region. J Quant Spectrosc Radiat Transf 2018;219:199–212. https://doi.org/10.1016/j.jqsrt.2018.07.022.

[11] Urban S, Klee S, Yamada KMT. Ground State Ro-inversional Transitions of 15NH3 in the Far-Infrared Region. J Mol Spectrosc 1994;168:384–9. https://doi.org/10.1006/jmsp.1994.1287.

[12] Fusina L, Di Lonardo G, Canè E, Predoi-Cross A, Rozario H, Herman M. The high resolution spectrum of $^{15}NH_3$ in the far-infrared: rotation-inversion transitions in the ground, ν_2=1, 2 and ν_4=1 states. J Quant Spectrosc Radiat Transf 2017;203:417–24. https://doi.org/10.1016/j.jqsrt.2017.01.021.

[13] Canè E, Di Lonardo G, Fusina L, Tamassia F, Predoi-Cross A. The $\nu_2 = 1$, 2 and $\nu_4 = 1$ bending states of $^{15}NH_3$ and their analysis at experimental accuracy. J Chem Phys 2019;150:94301. https://doi.org/10.1063/1.5088751.